

**PDFlib PLOP: PDF Linearization, Optimization, Privacy**

**Page inserted by evaluation version  
www.pdflib.com – sales@pdflib.com**

## Cell-Penetrating-Peptide-Coated Nanoribbons for Intracellular Nanocarriers\*\*

Yong-beom Lim, Eunji Lee, and Myongsoo Lee\*

The self-assembly of designed molecules is a powerful approach for the construction of novel supramolecular architectures.<sup>[1,2]</sup> Self-assembled nanostructures are finding growing use in biological applications, which include molecular detection, drug delivery, and gene delivery.<sup>[3–6]</sup> The most important points that can be considered in developing self-assembled biomaterials are the precise control of nanostructures, effective functionalization to suit for the specific bioapplications, and the biocompatibility of the building blocks. Of the many types of molecular building blocks, peptide-based building blocks have the advantage that their constituent amino acids are biocompatible and structurally diverse. The  $\alpha$ -helical,  $\beta$ -sheet, and hydrophobic interactions have been the main driving forces for the peptide assemblies and generally result in coiled-coil  $\alpha$ -helical peptide bundles,  $\beta$ -sheet peptide ribbons or tubes, and cylindrical micelles.<sup>[7–10]</sup> Besides the naturally occurring  $\beta$ -sheet peptides, such as  $\beta$ -amyloid, many artificial  $\beta$ -sheet peptides have been designed.<sup>[11]</sup> The design principle for most of the artificial  $\beta$ -sheet peptide sequences is the alternating placement of positively charged, hydrophobic, and negatively charged amino acids. The combination of attraction between oppositely charged amino acids and solvophobic interactions between hydrophobic amino acids is the driving force for the proper  $\beta$ -sheet hydrogen-bonding arrangement in which the formation of a bilayered peptide ribbon is most favorable. The bilayered ribbon is stabilized by the interactions between hydrophobic surfaces of each  $\beta$  tape, which then generates a hydrophobic interface inside the ribbon. We envisioned that the hydrophobic interface inside the ribbon is a suitable place to encapsulate hydrophobic molecules and can therefore be potentially used for drug-delivery applications. Herein, we report the surface functionalization of nanostructures with cell-penetrating peptides (CPPs) and the successful encapsulation of hydrophobic molecules inside the peptide nanoribbon structure while preserving the ribbon morphology (Figure 1).

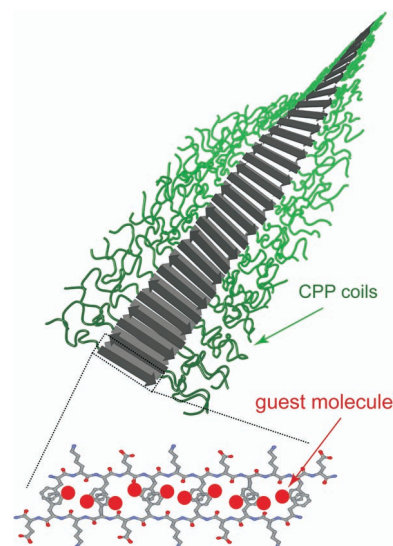


**Figure 1.** Representation of the nanoribbon formed by self-assembly of T $\beta$ P and encapsulation of hydrophobic guest molecules.

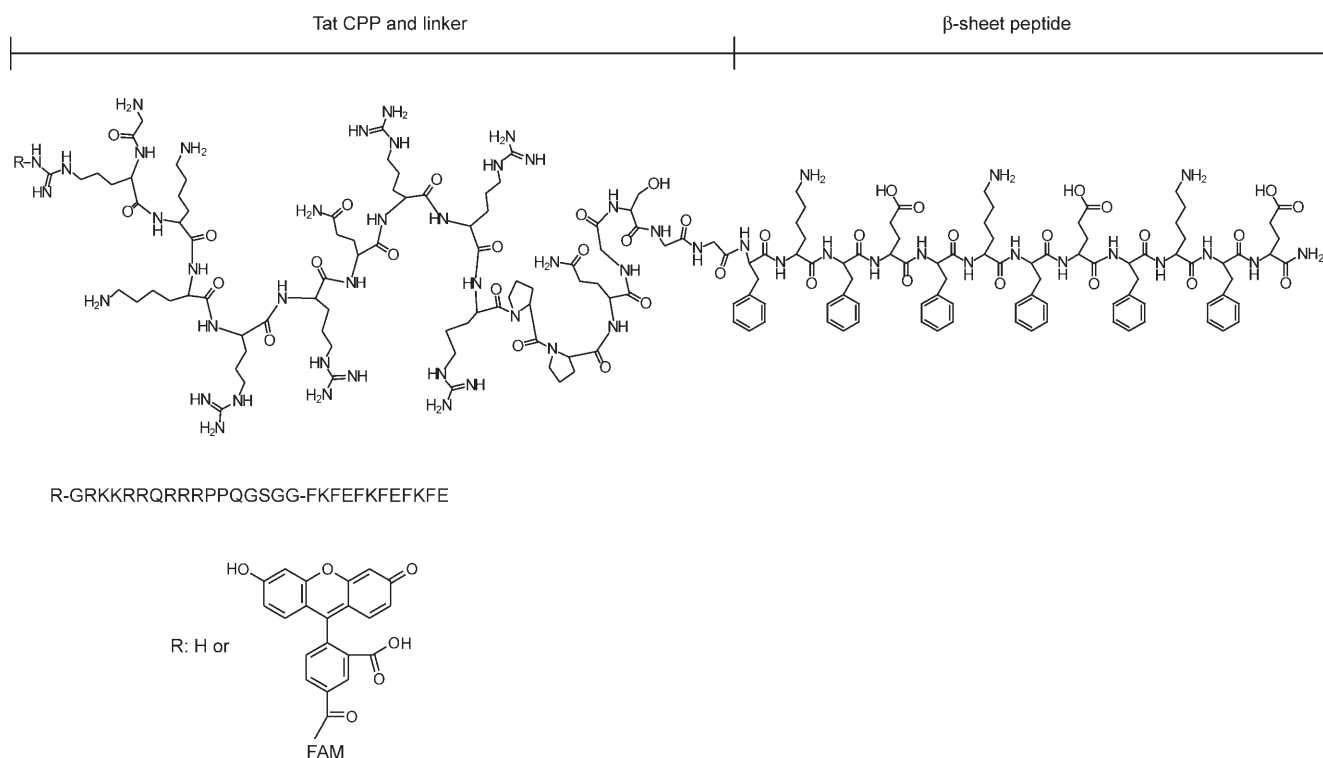
The peptide T $\beta$ P is designed for self-assembly and is composed of three functional blocks, a Tat CPP block (GRKKRRQRRRPPQ; Tat<sub>48–60</sub>), a flexible-linker block (GSGG), and a  $\beta$ -sheet assembly block (FKFEFKFEFKFE; Scheme 1). The CPPs consist of a short strand of amino acids that are capable of penetrating cell membranes.<sup>[12]</sup> Many cationic CPPs, including Tat CPP from human immunodeficiency virus type-1 (HIV-1) Tat protein, have been shown to efficiently cross the cytoplasmic membrane and the nucleus pore complex (NPC) barriers. The flexible-linker block was designed to decouple the Tat CPP block from the  $\beta$ -sheet assembly block, thereby minimizing undesirable interactions between them. The (FKFE)<sub>n</sub> sequence has been shown to form  $\beta$ -sheet-mediated nanostructures in which the bilayered ribbon is the most stable structure.<sup>[11a]</sup> The bilayer is stabilized by hydrophobic and  $\pi$ - $\pi$ -stacking interactions of phenylalanine residues on one face of the  $\beta$  tape (Figure 1).

The CD spectrum of T $\beta$ P in pure water showed a strong negative minimum at 201 nm and very weak minimum at 215 nm, indicating that random-coil structures are most prevalent and  $\beta$ -sheet formation is minimal (Figure 2a). These results indicate that both the Tat CPP and the  $\beta$ -sheet assembly blocks predominantly form random-coil structures in pure water. The Tat CPP is known to form a random-coil structure in solution.<sup>[13]</sup> We hypothesized that the well-known  $\beta$ -sheet assembly block in T $\beta$ P forms hardly any  $\beta$  sheets because of nonspecific electrostatic interactions between multiple positive charges at the Tat CPP block and multiple negative charges at the  $\beta$ -sheet assembly block, and the

[\*] Dr. Y.-b. Lim, E. Lee, Prof. M. Lee  
Center for Supramolecular Nano-Assembly and  
Department of Chemistry  
Yonsei University  
Seoul 120-749 (Korea)  
Fax: (+82) 2-393-6096  
E-mail: mslee@yonsei.ac.kr  
Homepage: <http://csna.yonsei.ac.kr>

[\*\*] We gratefully acknowledge the National Creative Research Initiative Program of the Korean Ministry of Science and Technology for financial support of this work.

Supporting information for this article is available on the WWW under <http://www.angewandte.org> or from the author.



**Scheme 1.** Structure and sequence of TβP peptides.

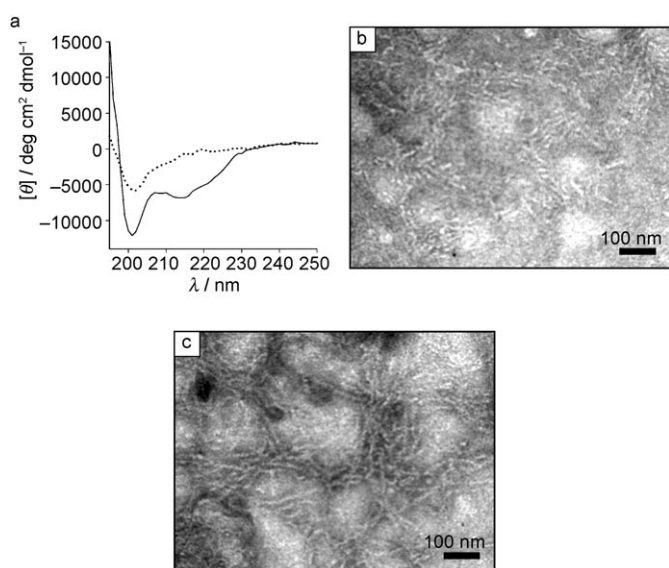


**Figure 2.** Self-assembly of TβP peptide. a) CD spectrum of TβP (50 μM) in pure water (dashed line) and in PBS buffer solution (solid line). b,c) A negatively stained TEM image of TβP in pure water (b) and PBS buffer solution (c).

hindrance in β-sheet formation by steric crowding of the bulky and flexible Tat CPP chain. We expected that the presence of salt in aqueous solution would screen the nonspecific charge interactions and strengthen hydrophobic interactions between the phenylalanine side chains.<sup>[14]</sup> The combined effects should enhance the formation of β-sheet

hydrogen bonds of TβP in salt-containing solutions. As shown in Figure 2a, the CD spectrum of TβP in phosphate-buffered saline solution (PBS; a physiological buffer) showed a clear minimum at 215 nm, which indicated that strong β-sheet interactions are induced upon the addition of PBS, which contains phosphates and about 150 mM of salts (NaCl and KCl). Detailed investigation with NaCl solutions of various concentrations led to the conclusion that the presence of salt is sufficient for the β-sheet formation of TβP. The CD signal for the β-sheet begins to increase starting from a NaCl concentration of around 10 mM (see the Supporting Information).

As expected, TEM investigation of TβP cast onto a TEM grid from pure water showed short cylindrical objects of less than 100 nm in length (Figure 2b). In contrast, a micrograph of TβP cast from PBS buffer solution revealed one-dimensional nanoribbons of more than several micrometers long and 6 nm wide (Figure 2c). These results clearly demonstrate that strong β-sheet interactions in a salt-containing solution enhance the self-assembly characteristics of TβP, resulting in efficient growth of the nanoribbon. It has been shown that β-sheet peptides usually form a hierarchy of supramolecular structures, tapes, ribbons, fibrils, and fibers.<sup>[11]</sup> Higher-order aggregates (fibrils and fibers) are formed by lateral aggregation of the elementary ribbons. To inhibit the formation of the higher-order aggregates, poly(ethylene glycol) (PEG) has been reported to be grafted onto a β-sheet peptide.<sup>[15]</sup> As TβP nanoribbons shown in Figure 2c exist as elementary ribbons, it is likely that the flexible Tat CPP block acted similarly to PEG and inhibited the lateral aggregation of the TβP nanoribbon. The results strongly indicate that TβP forms

well-separated nanoribbons in salt-containing solution with multiple Tat CPPs displayed on the surface (see Figure 1).

To investigate whether T $\beta$ P could encapsulate hydrophobic molecules at the inside of the ribbon structure, encapsulation experiments were performed with the hydrophobic fluorescent probes pyrene and nile red. The experiments revealed that T $\beta$ P can encapsulate both hydrophobic molecules. The ratio of the intensities of the first (371 nm) and the third (382 nm) peaks of the pyrene monomer,  $I_1/I_3$ , can be used to determine the polarity of the pyrene environment.<sup>[16]</sup> The measured  $I_1/I_3$  ratio of 0.8 for the pyrene encapsulated in T $\beta$ P indicates that the pyrene is located in the highly nonpolar microenvironment (Figure 3a). Furthermore, encapsulation

done in PBS buffer solution than in pure water (see the Supporting Information).

For studying intracellular delivery, T $\beta$ P was fluorescently labeled with carboxyfluorescein (FAM) at the N terminus (FAM-T $\beta$ P). T $\beta$ P and FAM-T $\beta$ P coassembled in a 50:1 ratio. This mixture was then added to mammalian cells and the internalization monitored by fluorescence-activated cell sorter (FACS) in which only fluorescence from live cells is gated. Before FACS was performed, the cells were treated with a sufficient amount of trypsin to disintegrate outer cytoplasmic membrane-bound peptides. The internalization efficiency of the T $\beta$ P nanoribbon was shown to be considerably higher than that of monomeric Tat CPP (Figure 4a).

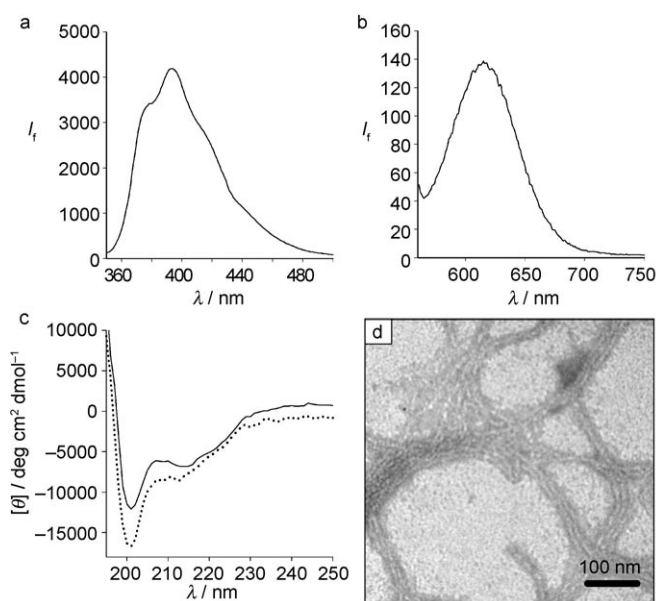


**Figure 3.** Encapsulation experiments. a) Fluorescence emission spectrum of T $\beta$ P encapsulated with 2 mol% pyrene (50  $\mu$ M in PBS buffer solution). Excitation was 336 nm. b) Fluorescence emission spectrum of T $\beta$ P encapsulated with 5 mol% nile red (50  $\mu$ M in PBS buffer solution). Excitation was at 550 nm. c) CD spectrum of T $\beta$ P (solid line) and T $\beta$ P encapsulated with 5 mol% nile red (dashed line). d) A negatively stained TEM image of T $\beta$ P encapsulated with 5 mol% nile red.  $I_f$ =fluorescence intensity.

of nile red in T $\beta$ P resulted in the strong fluorescence emission that is characteristic of nile red fluorescence in a nonpolar environment (Figure 3b). Nile red is a polarity-sensitive fluorescent probe that emits strong fluorescence only in a nonpolar environment.<sup>[17]</sup> The CD spectrum showed that the encapsulated molecules do not interfere with  $\beta$ -sheet formation (Figure 3c). TEM observation of nile red or pyrene encapsulated in T $\beta$ P revealed that the long ribbon structures are well preserved even after the incorporation of the guest molecules (Figure 3d). The ribbon structures appear to have grown slightly upon the addition of the fluorescent dye. All this evidence suggests that the hydrophobic guest molecules are intercalated between the hydrophobic interfaces formed by the stacking of two  $\beta$  tapes (Figure 1). Encapsulation efficiency was found to be higher when the experiment was

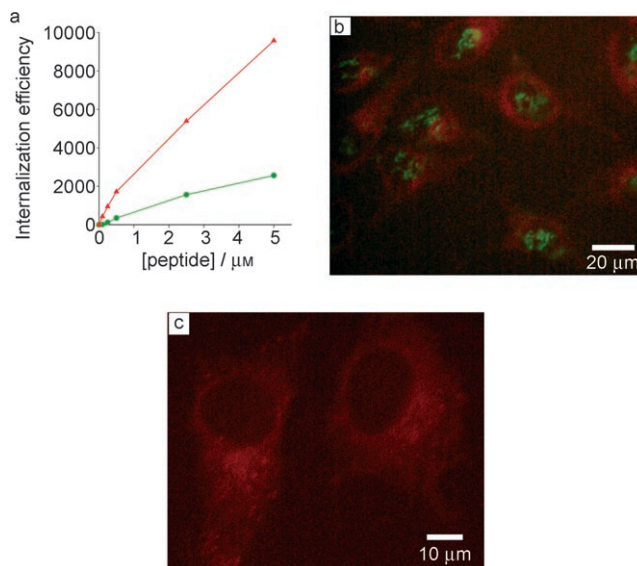


**Figure 4.** Cell-internalization study. a) Internalization efficiency analysis by FACS. Monomeric Tat CPP, green; T $\beta$ P nanoribbon, red. The abscissa represents a total peptide concentration (T $\beta$ P + FAM-T $\beta$ P). b) Overlaid CLSM image of cells treated with nile red encapsulated in the T $\beta$ P nanoribbon. T $\beta$ P, green; nile red, red. c) Intracellular distribution of nile red. HeLa cells were treated for 4 h. The total peptide concentration (T $\beta$ P + FAM-T $\beta$ P) was 5  $\mu$ M.

As the monomeric Tat CPP has a strong tendency to form a random-coil conformation, as described above, and does not have a  $\beta$ -sheet assembly block, it can be considered to exist in solution as separated peptide units. This result indicates that densely coated Tat CPP in the nanoribbon can penetrate cell membranes more efficiently than a single Tat CPP.<sup>[18]</sup>

Intracellular drug delivery of T $\beta$ P was investigated by confocal laser scanning microscopy (CLSM) after the encapsulation of nile red. Remarkably, most of the T $\beta$ P (green) are located in the nucleus and nucleoli, whereas nile red (red) is found exclusively in the cytoplasm (Figure 4b,c). The analogous experiment with pyrene encapsulation resulted in the same trend in the pattern of cellular distribution. We explain these results through the theory that upon entering into the cytoplasmic compartment through the cell-penetrating action of Tat CPP, the nanoribbon disassembles with simultaneous release of the encapsulated guest molecules, and the disassembled T $\beta$ P units are then further translocated into the

nucleus compartment as Tat CPP has a nucleus-localization signal. The hydrophobic Nile red molecules might be enriched in endoplasmic reticulum (ER) and/or mitochondrial membranes. Although the definitive mechanism of the disassembly in the cytoplasmic compartment is not clear at present, the cytoplasmic environment, a complex and very viscous (gel-like) solution with a myriad of proteins, nucleic acids, and chemicals, is likely to interfere with the proper  $\beta$ -sheet interactions of T $\beta$ P, thereby driving the nanoribbon to disassemble. Notably, the self-assembly behavior of T $\beta$ P is significantly dependent on the solution environment, such as the presence of salt (see Figure 2). Additional possibilities are that the peptide is proteolytically degraded or that the dye simply leaks out while the peptide remains intact in the cytoplasmic environment.

In conclusion, we have shown that hydrophobic interface inside the  $\beta$ -sheet peptide nanoribbon structure is a suitable place to encapsulate hydrophobic guest molecules and can be a promising high-efficiency drug-delivery vehicle when combined with CPPs. One can envision that this Tat-functionalized nanoribbon might be developed for the selective and simultaneous intracellular delivery of two different molecules, one into the nucleus and the other into the cytoplasm, in such a case where the one is conjugated by covalent bond to the peptide and the other is encapsulated.

Received: November 9, 2006

Revised: February 24, 2007

Published online: March 27, 2007

**Keywords:**  $\beta$  sheets · fluorescence · intracellular delivery · peptides · self-assembly

- [1] a) J. M. Lehn, *Proc. Natl. Acad. Sci. USA* **2002**, *99*, 4763–4768; b) T. Shimizu, M. Masuda, H. Minamikawa, *Chem. Rev.* **2005**, *105*, 1401–1443; c) J. A. A. W. Elemans, A. E. Rowan, R. J. M. Nolte, *J. Mater. Chem.* **2003**, *13*, 2661–2670; d) G. B. Ligthart, H. Ohkawa, R. P. Sijbesma, E. W. Meijer, *J. Am. Chem. Soc.* **2005**, *127*, 810–811.
- [2] a) M. Lee, B. K. Cho, W. C. Zin, *Chem. Rev.* **2001**, *101*, 3869–3892; b) W. Y. Yang, J. H. Ahn, Y. S. Yoo, N. K. Oh, M. Lee, *Nat. Mater.* **2005**, *4*, 399–402; c) B. S. Kim, D. J. Hong, J. Bae, M. Lee, *J. Am. Chem. Soc.* **2005**, *127*, 16333–16337.
- [3] S. I. Stoeva, J. S. Lee, J. E. Smith, S. T. Rosen, C. A. Mirkin, *J. Am. Chem. Soc.* **2006**, *128*, 8378–8379.
- [4] R. Savic, L. B. Luo, A. Eisenberg, D. Maysinger, *Science* **2003**, *300*, 615–618.
- [5] Y. Bae, S. Fukushima, A. Harada, K. Kataoka, *Angew. Chem.* **2003**, *115*, 4788–4791; *Angew. Chem. Int. Ed.* **2003**, *42*, 4640–4643.
- [6] K. K. Ewert, H. M. Evans, A. Zidovska, N. F. Bouxsein, A. Ahmad, C. R. Safinya, *J. Am. Chem. Soc.* **2006**, *128*, 3998–4006.
- [7] S. X. Ye, J. W. Strzalka, B. M. Discher, D. Noy, S. Y. Zheng, P. L. Dutton, J. K. Blasie, *Langmuir* **2004**, *20*, 5897–5904.
- [8] S. G. Zhang, *Nat. Biotechnol.* **2003**, *21*, 1171–1178.
- [9] S. Fernandez-Lopez, H. S. Kim, E. C. Choi, M. Delgado, J. R. Granja, A. Khasanov, K. Kraehenbuehl, G. Long, D. A. Weinberger, K. M. Wilcoxen, M. R. Ghadiri, *Nature* **2001**, *412*, 452–455.
- [10] J. D. Hartgerink, E. Beniash, S. I. Stupp, *Science* **2001**, *294*, 1684–1688.
- [11] a) D. M. Marini, W. Hwang, D. A. Lauffenburger, S. G. Zhang, R. D. Kamm, *Nano Lett.* **2002**, *2*, 295–299; b) G. T. Dolphin, P. Dumy, J. Garcia, *Angew. Chem.* **2006**, *118*, 2765–2768; *Angew. Chem. Int. Ed.* **2006**, *45*, 2699–2702; c) A. J. Baldwin, R. Bader, J. Christodoulou, C. E. MacPhee, C. M. Dobson, P. D. Barker, *J. Am. Chem. Soc.* **2006**, *128*, 2162–2163; d) C. W. G. Fishwick, A. J. Beevers, L. M. Carrick, C. D. Whitehouse, A. Aggeli, N. Boden, *Nano Lett.* **2003**, *3*, 1475–1479; e) A. Aggeli, M. Bell, L. M. Carrick, C. W. Fishwick, R. Harding, P. J. Mawer, S. E. Radford, A. E. Strong, N. Boden, *J. Am. Chem. Soc.* **2003**, *125*, 9619–9628.
- [12] S. Futaki, *Adv. Drug Delivery Rev.* **2005**, *57*, 547–558.
- [13] R. Tan, A. D. Frankel, *Proc. Natl. Acad. Sci. USA* **1995**, *92*, 5282–5286.
- [14] T. Ghosh, A. Kalra, S. Garde, *J. Phys. Chem. B* **2005**, *109*, 642–651.
- [15] a) T. S. Burkoth, T. L. S. Benzinger, D. N. M. Jones, K. Hallenga, S. C. Meredith, D. G. Lynn, *J. Am. Chem. Soc.* **1998**, *120*, 7655–7656; b) J. Hentschel, E. Krause, H. G. Börner, *J. Am. Chem. Soc.* **2006**, *128*, 7722–7723.
- [16] K. Kalyanasundaram, J. K. Thomas, *J. Am. Chem. Soc.* **1977**, *99*, 2039–2044.
- [17] A. P. Goodwin, J. L. Mynar, Y. Z. Ma, G. R. Fleming, J. M. J. Fréchet, *J. Am. Chem. Soc.* **2005**, *127*, 9952–9953.
- [18] M. Sung, G. M. K. Poon, J. Gariépy, *Biochim. Biophys. Acta Biomembr.* **2006**, *1758*, 355–363.